Sensors and Actuators B 181 (2013) 424–431

Contents lists available at SciVerse ScienceDirect

Sensors and Actuators B: Chemical

journal homepage: www.elsevier.com/locate/snb

A highly selective chemical sensor array based on nanowire/nanostructure for gas identification

Yushi Hu[a], Hyunjoong Lee[b], Suhwan Kim[b], Minhee Yun[a,c,*]

[a] Department of Electrical and Computer Engineering, Swanson School of Engineering, University of Pittsburgh, Pittsburgh, PA 15261, USA
[b] Department of Electrical Engineering, Seoul National University, Seoul 151-744, Republic of Korea
[c] Department of Bioengineering, Swanson School of Engineering, University of Pittsburgh, Pittsburgh, PA 15261, USA

ARTICLE INFO

Article history:
Received 6 April 2012
Received in revised form
19 December 2012
Accepted 29 January 2013
Available online xxx

Keywords:
Single nanowire
Nanowire array
Nanoelectronics
Sensor circuit

ABSTRACT

Real-time detection and identification of multiple gases based on a single-nanowire sensor array have been investigated. We present the fabrication, characterization, and sensing performance of a single-nanowire array consisting of four different materials from three categories, which are metal (palladium), conducting polymer (polypyrrole and polyaniline), and semiconductor (zinc oxide), on a chip via a site-specific electrochemical deposition process. The presented nanowire array on a single chip has been used to detect and identify four target gases including hydrogen, methanol, carbon monoxide, and nitrogen dioxide. Each single nanowire shows an excellent sensitivity at room temperature, and a sub-ppm (parts per million) detection limit is achieved. The identification of these four targets has been successfully demonstrated with the help of principal component analysis. Our study shows that this single-nanowire sensor array is able to not only accurately distinguish four targets but also roughly estimate the target concentration, forming a basis for an electronic nose with far-reaching applications.

1. Introduction

An electronic nose (e-nose) that mimics the olfaction system in mammals is expected to be applied to a wide range of areas, such as disease diagnosis, food quality inspection, gas chromatography, and spacecraft atmospheric monitoring [1–5]. These applications require that the e-nose not only detects an individual target at extremely low concentration (down to ppm or lower), but also identifies the exact chemicals of the target with high selectivity. In order to improve sensitivity, previous studies employed nanomaterials, such as nanowires and nanoparticles, as e-nose building blocks because of their high surface area to volume ratio and superior sensitivity for detecting volatile organic compounds (VOCs) and toxic industrial gases (e.g., NO_2 and CO) [6,7]. Target identification, on the other hand, was mainly realized by including an array of different sensor elements to build a sensor array as the base for the e-nose device [8,9].

Despite previous success in gas detection, the reported sensor array based e-noses suffer from several drawbacks that seriously limit their applications. First, the active materials in the sensor elements are usually limited to one type of material, such as metal oxides and conducting polymers [7–9]. This limitation restricts the variety of sensible target molecules of the sensor array, thus rendering it a device only applicable to specific targets. In addition, the similar chemical properties among the active sensing materials in the array can result in a less than optimal selectivity. For example, a reported sensor array based on only conducting polymer nanowires failed to clearly identify two of the target VOCs [10]. Second, the previous nano sensor array studies were satisfied with distinguishable sensing patterns but did not attempt to verify the sensor performance in real situations or explore the possibility of concentration estimation. For advanced cases, such as spacecraft monitoring, where both the compositions and the concentrations of targets need to be identified, the ability of the sensor array to estimate the target concentration becomes extremely important.

In this work, we present a site-specific electrochemical deposition method to incorporate an array of single nanowires on a single chip. The incorporation of four single nanowires – palladium (Pd), polypyrrole (PPy), polyaniline (PANI), and zinc oxide (ZnO) – from three material types – metal, conducting polymer, and metal oxide – into a sensor array is demonstrated for the first time. The developed sensor array in this research is able to detect four gases with distinct properties, including carbon monoxide (CO, a very common household toxic gas), hydrogen (H_2, an important potential energy source), methanol (CH_3OH, a representative VOC), and nitrogen oxide (NO_2, a common oxidizing gas and a common industrial toxic gas), and well-separated sensing patterns are built up with the help of principal component analysis (PCA) for all targets, even at

* Corresponding author at: Department of Electrical and Computer Engineering, Swanson School of Engineering, University of Pittsburgh, Pittsburgh, PA 15261, USA. Tel.: +1 412 648 8989; fax: +1 412 624 8003.
E-mail address: yunmh@engr.pitt.edu (M. Yun).

0925-4005/$ – see front matter © 2013 Elsevier B.V. All rights reserved.
http://dx.doi.org/10.1016/j.snb.2013.01.084

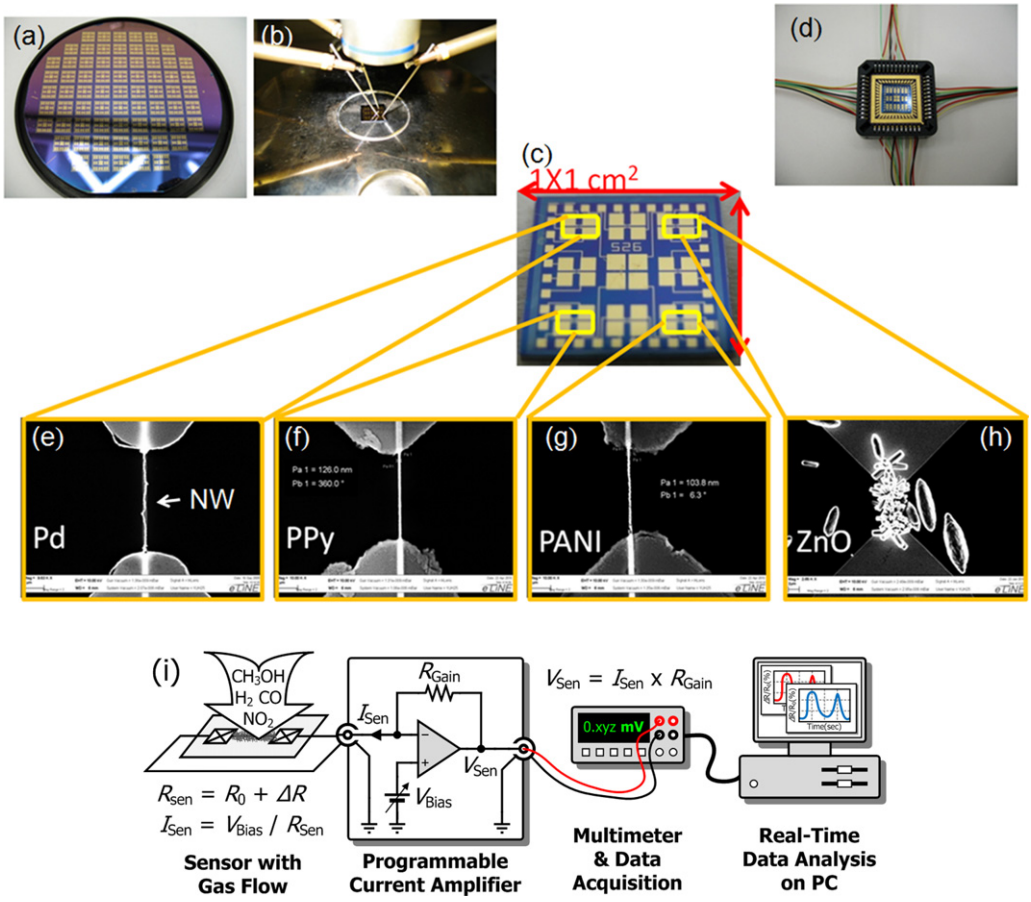

Fig. 1. Nanowire fabrication process and SEM images of synthesized single nanowires. (a) 4-in. Si wafer containing 69, 1 cm × 1 cm chips. (b) A chip placed under three probes of a probe station during nanowire electrochemical deposition. (c) Chip containing four different single nanowires. (d) Sensor chip built on a chip with a single-nanowire array after wire bonding and integration. (e–g) SEM images of Pd, PPy, and PANI single nanowires, respectively. The bright thin line denotes the nanowire, and the bright areas on top and bottom denote Ti/Au electrodes. (h) SEM image of ZnO nanowire. (i) Measurement setup for the read-out of sensor signal.

extremely low (sub-ppm) concentrations. Finally, a blind experiment where the sensor array was exposed to four gas injections with unknown compositions and concentrations was conducted to verify the identification ability. We found that, by comparing each injected target with the original sensing patterns, the target composition can be successfully identified and, moreover, approximated with the accuracy determined by calibration (data collected to build up sensing patterns) PCA data point density. Therefore, the sensor array synthesis and systematic analysis performed here not only provide a feasible way of incorporating nanowires from different material types on a single chip, but also point out a way for target concentration estimation through PCA.

2. Experimental

2.1. Template preparation and nanowire synthesis

The single Pd, PPy, and PANI nanowires were electrochemically deposited inside predefined PMMA nanochannels on top of a silicon (Si) chip. A p-type 4-in. Si wafer with a thin layer of SiO_2 (100 nm thick) was chosen as the substrate. After photolithography and e-beam evaporation, a total of 69 chips of 1 cm × 1 cm size were defined on top of the wafer, and each chip consisted of 16 pairs of Ti/Au working electrodes and 4 Ti/Au gate electrodes. A layer of 100 nm thick PMMA was then spun on the wafer surface, while e-beam lithography was used to direct-write single nanochannels with adjustable width (typically less than 100 nm) across each Ti/Au working electrode pair. Because the distance between the working electrodes decides the actual length of nanochannels, both the width and length of the nanochannels can be predefined.

2.2. Nanowire synthesis

Fig. 1 illustrates the fabrication process of a nanowire sensor array on a chip. After template preparation, the 4 in. wafer with patterned electrodes and nanochannels (Fig. 1(a)) are cut into small slices, and four different single nanowires are grown electrochemically with a probe station (Fig. 1(b)) on top of these 1 cm × 1 cm chips (Fig. 1(c)) using different electrolyte solutions. Each chip had 16 pairs of working electrodes with one nanochannel across each pair. Four gate electrodes were positioned in the center of the chip to maximize the field effect. The purpose of adding gate electrodes was to better control the nanowire growth by applying a vertical electric field underneath the channel, as discussed in our previous studies [11,12]. A probe station (Micro Manipulation Co. Inc.) with three probes was used to make direct contacts with the electrodes. Two of the probes were connected with a pair of working electrodes, while the third one was connected with one of the gate electrodes. A small drop of electrolyte solution was placed on top of the nanochannel, while a semiconductor analyzer (Agilent B1500A) was employed to provide a constant current signal through the working electrodes and a constant voltage signal through the gate electrode. No heating element was used during growth and growth temperature was kept at room temperature (27 °C). Once the nanowire growth was complete, all the electrical signals were turned off, and the remaining solution was blown

away. After the electrochemical growth, each chip with four single nanowires is assembled into a sensor device with external electrical connections (Fig. 1(d)). The electrolyte solutions for the nanowires were: Pd:$Pd(NH_2)_2(NO_2)_2$ (diaminepalladium nitrite) (10 g/L) and $NH_4SO_3NH_2$ (ammonia sulfamate) (100 g/L); PPy:NaCl (0.2 M) and pyrrole (98%, 0.1 M); PANI:HCl (0.1 M) and aniline (98%, 0.01 M); ZnO:$ZnCl_2$ (0.005 M) and NaCl (0.015 M). The growth of the Pd (Fig. 1(e)), PPy (Fig. 1(f)), PANI (Fig. 1(g)) single nanowires was completed via electrochemical deposition, while the ZnO nanowire growth (Fig. 1(h)) was completed via an electrochemical deposition followed by a hydrothermal treatment. In the hydrothermal treatment, the chip with an electrochemically grown ZnO nanowire was immersed into a solution (0.05 M $Zn(NO_3)_2$ and 0.05 M HTMA) that was heated up to 90 °C for 30 min to fully oxidize the as-deposited ZnO nanowire. All of the chemicals were purchased from Sigma Aldrich Inc.

2.3. Sensor and characterization setup

The chip with four different single nanowires was rinsed in DI water and dried before they were stabilized on top of a 44 pin ceramic chip holder. A wire bonder was used to wire each pair of working electrodes to the external circuit. This chip holder was plugged into a PLCC 44 socket (Fig. 1(d)), which was directly connected to sensor input and output circuits. The gas flow system was built on an MKS mass flow controller (647C) and several mass flow meters (1179A). Pure nitrogen (N_2 99.999%) was used as both carrier gas and dilution gas in the test. It is also used to simulate the ambient conditions. Factory-certified hydrogen (H_2: 10% and 0.1%), nitrogen dioxide (NO_2: 10 ppm), and carbon monoxide (CO: 2000 ppm) were purchased, and methanol (CH_3OH) was generated by a homemade vapor generator, which is based on a dip-in tube set-up using a glass Buchner funnel bubbler (refer to Supplementary Material for details on the vapor generator). These target source gases were diluted by pure N_2 to a desired concentration during gas detection. Fig. 1(i) illustrates a circuit diagram of electrical measurement setup for the electrical signal readout system from the sensor array, consisting of a programmable current amplifier (Keithley 428), a data acquisition system with multimeter (Keithley 2701), and a PC with real-time data analyzing program (LabVIEW). In this configuration, the current amplifier provides a bias voltage of ~17 mV (V_{Bias}), reads the current signal across each nanowire, and converts it into voltage signal with an adjustable amplification factor of R_{Gain}. The voltage signal is then measured by the data acquisition system and analyzed using a LabVIEW program after converting voltage signal into resistance signal. This customized LabVIEW program was designed to accurately control the gas flow rate and plot the real-time resistance signal of each nanowire. In this manner, the sensor's current signal which is weak and vulnerable to the environmental noise can be robustly measured using a current amplifier, instead of being directly measured.

3. Results and discussion

Scanning electron microscopy (SEM) is used to investigate the morphology of the four single nanowires, and the results are illustrated in Fig. 1(e)–(h). The diameters of the Pd, PPy, and PANI single nanowires illustrated in Fig. 1(e)–(g) are 128 nm, 126 nm, and 104 nm, respectively, and the nanowires are uniform along the length of the channel with both ends well connected with the electrodes, demonstrating that the growth of the nanowires is well confined by the 100 nm wide and 5 μm long nanochannels. It should be noted that each chip is composed of 16 electrode pairs. Thus, up to 16 different single nanowires can be integrated onto the same chip by choosing the proper electrolyte solutions, providing a superior expansibility for future development.

The growth of the ZnO nanowire, unlike that of the Pd and conducting polymer nanowires, is much less affected by the electric field than by the substrate conditions [13]. Previous attempts to fabricate ZnO nanowires laterally using hydrothermal processes [14,15] are not readily compatible with the synthesis of other materials either because of the prerequisite of a seed layer or requirements for the substrate crystal structure. Different from the ZnO nanowire, the zinc (Zn) nanowire can be easily obtained through electrochemical deposition at room temperature [16]. In this work, the Zn nanowire is first deposited into the predefined nanochannel via electrochemical deposition at room temperature, and a hydrothermal process is subsequently used to oxidize Zn into ZnO. Fig. 1(h) shows that the fabricated ZnO nanostructure is a nanorod bundle that consists of individual nanorods with diameters around 500 nm, and the width of the bundle is around 2.5 μm. The growth of the ZnO nanowire bundle is limited along the channel across the electrodes due to the limited growth sites provided by the electrochemically deposited Zn nanowire. As a result, the site-specific lateral growth of the single ZnO nanostructure is realized, although further improvement is needed to better limit its size.

In order to verify the chemical compositions of these nanowires, we employed energy dispersive X-ray spectroscopy (EDX) to characterize Pd and ZnO nanowires and Raman spectroscopy (Raman) to characterize PPy and PANI nanowires. The EDX spectrums (supplementary material, Fig. S1) showed clear Pd peak for the Pd nanowire and Zn and O peaks for the ZnO nanowire, demonstrating the successful formation of the Pd and ZnO nanowires. The characteristic peaks in the Raman spectrums for PPy and PANI also matched the values reported by previous studies [17–20], demonstrating the successful fabrication of PANI and PPy nanowires.

The chip with four single nanowires is then inserted into a gas sensing system as described in Section 2. The real-time resistances of four single nanowires can be monitored simultaneously using a multiplexer. When each nanowire is exposed to target gases, its resistance is subject to change because of chemical reactions or physical adsorptions/absorptions on the nanowire surface. We present this resistance change in a widely accepted normalized format, relative sensor response (RS), which can be defined as $RS = (R - R_0)/R_0 \times 100\%$. R and R_0 represent the nanowire resistances when exposed to a target gas and ambient conditions, respectively.

In order to investigate the sensing behavior of each sensor material, four targets (CO, CH_3OH, H_2, and NO_2) with concentrations spanning over two orders of magnitude are introduced into the array. Fig. 2 presents the real-time responses from four sensor elements when exposed to four target gases at different concentrations. Each row demonstrates the response for one target gas, while each column demonstrates the response from one sensor element. In this work, complete real-time responses for consecutive gas injection-purge cycles were used to provide information on both sensitivity and reproducibility. As shown in the first row of Fig. 2, the Pd nanowire is very sensitive to H_2 with the lowest detection limit at 94 ppm, although a 2 ppm detection limit was demonstrated in our previous study [21]. The downgrade of sensitivity may be due to the higher noise level introduced by the multiplexer during multichannel simultaneous monitoring. In contrast, the Pd nanowire has limited sensitivities to CH_3OH (one order of magnitude lower than for H_2), and it is almost completely insensitive to CO or NO_2. This conforms to the fact that Pd is highly selective and specific to H_2 detection [22]. The second row shows that, the PPy nanowire has similar sensitivities to all four gases. In the third row, the PANI nanowire shows high sensitivities to

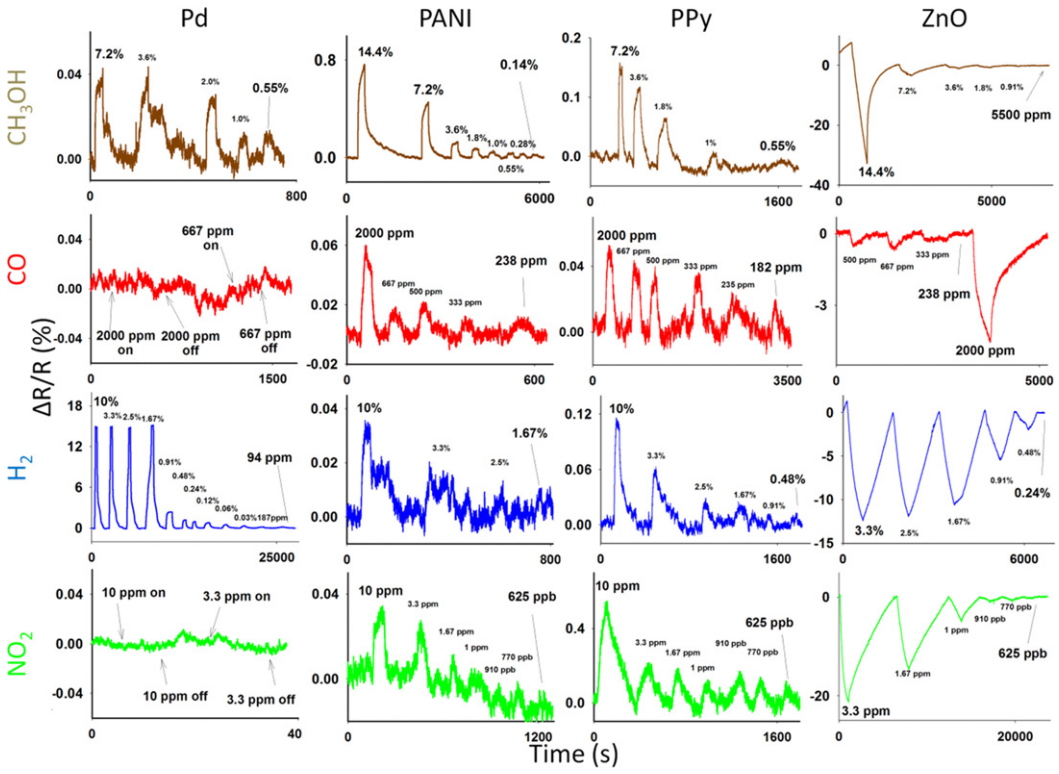

Fig. 2. Real-time sensing signals from four single nanowires for four target gases at different concentrations. The *x*-axis is time (s), and the *y*-axis represents RS ($\Delta R/R \times 100\%$). The rectangular in each graph represents the duration of each target gas injection, and the percent value on top of each rectangular represents the concentration of the target gas. Each sensing signal includes several gas injection/purge cycles at different concentrations.

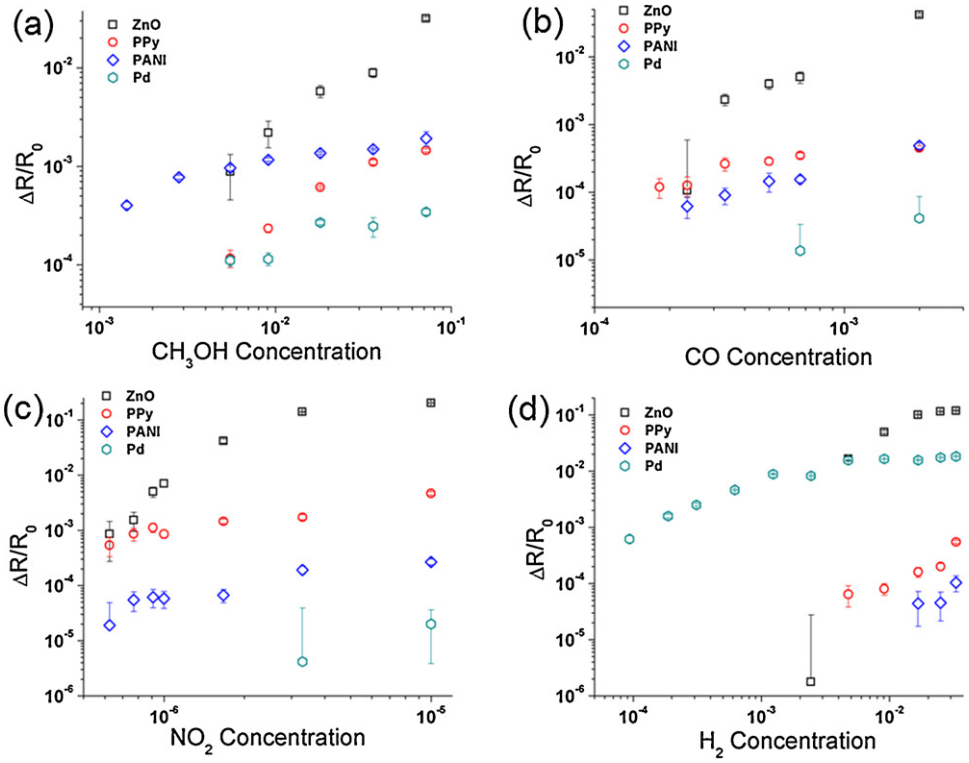

Fig. 3. Relationships between gas concentrations and relative sensitivities. Summarized data for (a) CH_3OH, (b) CO, (c) NO_2, and (d) H_2 with regard to different nanowire materials presented in four plots. In each plot, the x axis is gas concentration in logarithmic form, and the y axis represents RS in logarithmic form [log(RS)]. Due to the minus sign of the RSs from ZnO, ZnO's relative sensitivities are plotted using absolute values. The error bars represent the standard deviation due to the noise level in each gas injection.

CH_3OH and median sensitivities for the remaining three gases. These results are expected because PPy and PANI are well-known sensors for VOCs [9], and their sensitivities to CO, H_2, and NO_2 have also been reported. The sensing mechanisms of PANI and PPy are very similar; the introduction of small molecules into the polymer matrix blocks some of the conducting path and results in an increased resistance [23]. The sensing mechanism for NO_2 is more complicated and involves reduction/oxidation reactions [24]. Different from the Pd, PPy, and PANI nanowires, the ZnO nanowire is very sensitive to all four targets, showing considerably larger sensitivity in the last row of Fig. 2. Our findings match the fact that ZnO is able to sense a wide range of targets with relatively high sensitivity [25,26]. One thing worth mentioning is that, ZnO gas sensors normally show an increased resistance when exposing to oxidizing gases such as NO_2 and O_2, considering the n-type conduction nature of ZnO nanostructures [27]. However, our sensor showed a decreased resistance when NO_2 was introduced. A possible mechanism related to an N–P transition in ZnO nanostructure when it was exposed to NO_2 has been proposed by Wang et al., although more in-depth research is needed to fully understand this phenomenon [28]. Clearly, these four different nanowires show different sensing patterns for the target gases, providing a solid foundation for target gas identification. It should be noted that the response times from some nanowires (e.g., ZnO nanowire) were considerably long. The nanowire size is believed to be an important factor impacting the sensor response time. In theory, the smaller the nanowire is, the faster the nanowire gets saturated by the target gas either on the surface or in the bulk. As a result, a further reduction of the nanowire size down to sub-50 nm range may help reduce the response time. Other factors that may play a role in the response time include temperature and pressure. A higher sensing temperature of the sensor or the sensing environment can effectively increase the reaction rate, thus improve the response speed of the sensors.

The concentration-dependent responses shown in Fig. 2 not only provide insights into the sensing mechanisms for different sensor materials, but they also set up a relationship between signals and target concentrations, forming a basis for concentration estimation. To clearly express the concentration-signal relationship and to provide direct comparisons among nanowires, we plot the RSs against target concentrations in a logarithmic form in Fig. 3. Each plot corresponds to one target gas, and the RSs of the four nanowires are compared. In Fig. 3(a), for CH_3OH, the ZnO nanowire shows the highest sensitivity, and the Pd nanowire shows the lowest sensitivity. The PANI nanowire shows a slightly higher sensitivity than the PPy nanowire. In Fig. 3(b), for CO, the ZnO nanowire shows the highest sensitivity, and the PPy nanowire shows a slightly higher sensitivity than the PANI nanowire. The Pd nanowire has almost no sensitivity to CO. In Fig. 3(c), for NO_2, the ZnO nanowire has the highest sensitivity, and PPy has a higher sensitivity than the PANI nanowire. The Pd nanowire has almost no sensitivity to NO_2. In Fig. 3(d), in the case of H_2, the Pd and ZnO nanowires show similar sensitivity at high H_2 concentration. But the Pd nanowire remains highly sensitive to H_2 even at a very low H_2 concentration, while the sensitivity of the ZnO nanowire decreases sharply when the H_2 concentration drops. Neither the PPy nor PANI nanowire shows a high sensitivity to H_2. This again proves that the Pd nanowire is the most efficient in H_2 detection. By comparing the four plots, we can conclude the following: (i) this nanowire array is able to detect all four targets with the lowest detectable concentrations of CH_3OH, CO, H_2, and NO_2 at 1400 ppm, 182 ppm, 94 ppm, and 625 ppb (parts per billion), respectively; (ii) the sensing patterns of the different nanowires are completely different; and (iii) the sensing signals are closely related to the target concentration. The disparity in the sensing patterns is utilized for gas identification, and the concentration-dependent sensing response provides the basis for target concentration estimation. It is also noticed that the PPy and PANI nanowires have similar sensing patterns as compared to the ZnO and Pd nanowires. This infers that, although chemically different, nanowires from the same material type possess similar sensing patterns, which suggests that adding different material types to the nanowire array could increase selectivity.

A method that can clearly classify the different target gases and predict both the composition and concentration of an unknown target gas is needed. PCA is a popular tool in e-nose signal processing and recognition and has been employed widely in previous studies [1,6,8]. PCA reduces the dimensions of data by constructing a new set of orthogonal bases (i.e., principal components or PCs) that enable compact representations of the original data. In other words, PCA focuses on the distinct features among individual nanowires while eliminating the redundant and repetitive information. In this work, the saturated RS values of each nanowire when exposed to a certain target under certain concentration are extracted, and the four nanowires constitute four data sets with each data point denoting the saturated RS for a target at a concentration. PCA is then used to reduce the four-dimensional data to a two-dimensional (2D) or three-dimensional (3D) space whose bases are the first two or three principal components with the largest variances. This new data

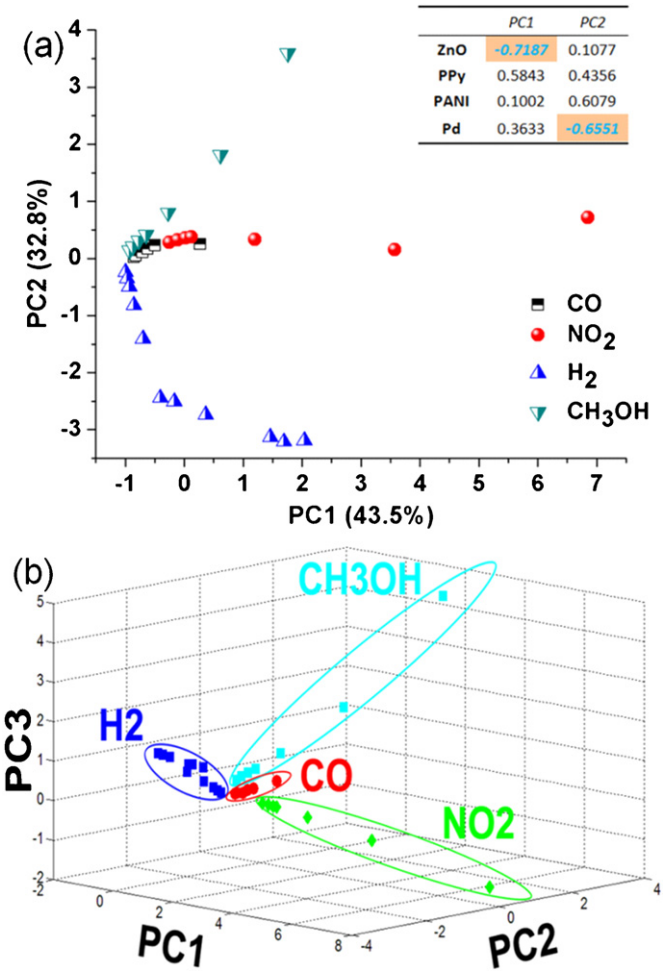

Fig. 4. Data clustering plots via PCA for the four-nanowire sensor array. (a) 2D PCA plot formed using the first two PCs (PC1 and PC2) shows clear clustering for data points from each of the four gas targets at high concentrations although data points at lower concentrations appear to be closely located. Inset: corresponding correlation matrix for PC1 and PC2 in (a). (b) 3D PCA map using the first three PCs (PC1, PC2, and PC3) shows a 3D view of the data points for all four target gases.

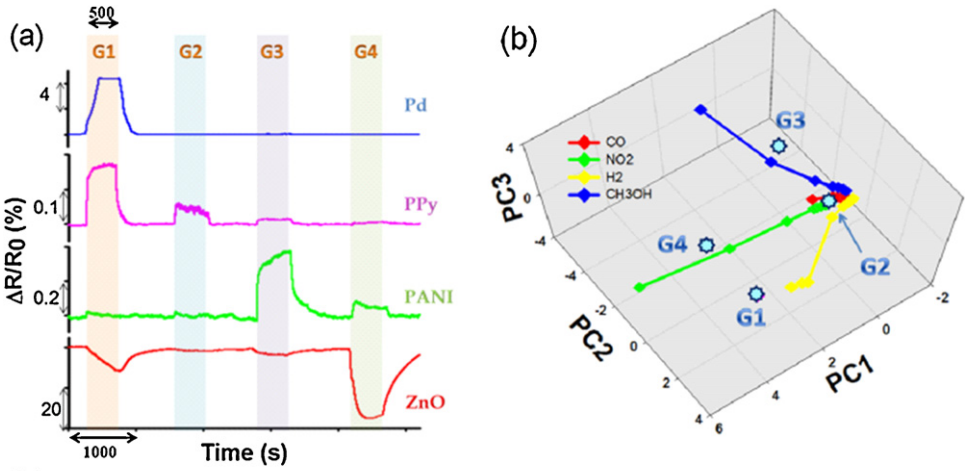

(c)

	Gas 1	Gas 2	Gas 3	Gas 4
Real composition (concentration)	H2 (2%)	CO (400 ppm)	CH3OH (5.4%)	NO2 (5 ppm)
Estimated composition (concentration)	H2 (≈7.2%)	CO (≈667 ppm)	CH3OH (≈3.6%)	NO2 (≈3.3 ppm)

Fig. 5. Real-time sensing signals and the corresponding PCA plot for a blind experiment consisting of four 'unknown' gas injections. (a) Real-time signals collected from the four-nanowire array when the device is exposed to four consecutive gas injection-purge cycles. The four gas injection events are marked as G1, G2, G3, and G4, and each gas injection lasts for a period of 500 s followed by an introduction of pure N_2 into the chamber to purge the target gases. (b) 3D scattering plot via PCA includes both the smell prints and points for the four new gas injection events, which are marked as octagons and labeled G1, G2, G3, and G4. (c) Comparison between real gas conditions and estimated conditions by the e-nose. The real compositions and concentrations (presented in parentheses) are listed above the estimated compositions and concentrations for a clear comparison.

matrix can be plotted in a 2D or 3D format for easy visualization, with each data point representing a certain gas under a certain concentration, and its coordinates are the scores with regard to each PC.

Fig. 4(a) and (b) illustrates the 2D and 3D PCA plots from this four-nanowire sensor array. The variances possessed by the principal components are 41.8% (PC1), 36.7% (PC2), 18.5% (PC3), and 3.00% (PC4). In Fig. 4(a), data points from NO_2, CO, H_2, and CH_3OH aggregate in different areas, which can be assigned as the specific sensing patterns for these targets. However, differentiation between CO and NO_2 at lower concentrations is difficult in this plot. Fig. 4(b) shows a clearer view by adding PC3 to build a 3D plot. The total variance explained in this 3D plot is increased to 97%, thus almost all of the information is demonstrated. In this plot, NO_2 and CO data points are clearly separated, and thus the sensing patterns of the four gases are distinguishable even at the lowest detected concentration (625 ppb for NO_2). One thing worth mentioning is the contribution from the Pd and ZnO nanowires. According to the PCA coefficient matrix, shown in the inset of Fig. 4(a), ZnO and Pd provide the most distinct coefficients for PC1 and PC2, respectively. The difference between the coefficients from PANI and PPy, on the other hand, is much smaller. This indicates that ZnO and Pd provide unique properties to this array, proving the idea that materials from different types are favorable in the e-nose application. Overall, we are able to successfully specify the sensing patterns for NO_2, CO, H_2, and CH_3OH down to a ppb concentration level by using the sensor array consisting of the ZnO, PPy, PANI, and Pd nanowires.

After building up distinguishable sensing patterns, we furthered the research by investigating the reliability of this sensor array in actual gas identification in a blind experiment. A blind experiment is conducted where we inject a target gas into the sensing chamber without knowing its composition or concentration, and estimate the gas type and concentration based on the real-time electrical signals from the nanowire array. Although overlooked in previous studies, this step is crucial for the following reasons. (i) It eliminates the bias of the observer due to prior knowledge of the expected result, improving the credibility of the observed results. (ii) It mimics the real operation condition and verifies the performance of the device by repeating the experiment and reassuring its reliability. Fig. 5(a) presents a blind experiment sensing data that consists of real-time signals from four consecutive unknown gas injections. Each of the injected gas is one of the four target gases with arbitrary concentration. Pure nitrogen was used to purge the injected gas for 500 s before the injection of next gas. The saturated RS values from the four nanowires for each gas injection are processed by the PCA procedure mentioned above. After PCA, each gas injection corresponds to a new data point on the original PCA plot with sensing patterns, as shown in Fig. 5(b). Although the data points for low concentration gases are crowded, they are clearly separated in a zoomed view (supplementary material, Fig. S2). Based on the relative position between the injection data point and the sensing patterns, the composition and concentration of each injected gas can be estimated. Gas 4, for example, has a corresponding data point closest to the point for 3.3 ppm NO_2, so the best estimate for gas 4 is NO_2 with a concentration of 3.3 ppm. It is worth mentioning that the accuracy of the concentration estimation depends on the resolution of the concentration in the original sensing patterns. That is, by adding more calibration data points with intermediate concentrations into the sensing patterns, concentration estimation with better accuracy can be achieved. Similarly, the estimated compositions and concentrations for gases 1, 2, and 3 are 7.2% H_2, 667 ppm CO, and 3.6% CH_3OH, respectively. Although the position of the data point for gas 2 is not clearly shown in Fig. 5(b), a zoomed PCA plot shows that this point sits closest to the point for 667 ppm CO. Fig. 5(c) compares the actual and estimated gas compositions and concentrations to verify the estimation accuracy. As demonstrated, the compositions of all four injected gases are correctly estimated, demonstrating the identification ability of this nanowire array. The estimated concentrations are close to the actual values, although their accuracy can be further improved by increasing the number of calibration data points in the sensing patterns. Verified by the

blind experiments, this sensor array not only successfully identified the four target gases but also provided rough estimations for the target concentrations.

4. Conclusions

In summary, we successfully fabricated, and demonstrated a sensor array consisting of four different single nanowires, Pd, PPy, PANI, and ZnO, site-specifically using electrochemical deposition. The structure of these single nanowires was characterized using SEM, and the properties were confirmed using EDX and Raman spectroscopy. The 1 cm × 1 cm chip with the four-nanowire array on top was integrated into a sensing system, and four different target gases, including H_2, CH_3OH, CO, and NO_2, were selected for identification. With the help of PCA, the sensing patterns for all four target gases were successfully built up without overlap even at extremely low concentration levels (625 ppb). In addition, a blind experiment verified the identification ability of the nanowire sensor array and provided rough estimations of target concentrations, although further development is needed to improve the accuracy. It is necessary to emphasize that we can potentially synthesize up to 16 different single nanowires site-specifically on the chip, greatly improving the target range and the identification ability of this sensor array. It should also be noted that this work employed pure dry N_2 as carrier gases and more study is needed to investigate the impact of humidity on the individual sensors. To sum up, this work demonstrated the fabrication of a single-nanowire/nanostructure array that can be used for target concentration estimation through principal component analysis, opening up the possibility of developing a widely applicable e-nose system that identifies both the composition and the concentration of the target gases.

Acknowledgements

The authors gratefully acknowledge X. Luo for the EDX analysis and I. Lee for the Raman spectroscopy analysis. The authors are also grateful to Z. Mao and D. Perello for help with data analysis. This work was supported by the National Science Foundation (NSF-ECCS 0824035) and the Mascaro Center for Sustainable Innovation (MCSI). Minhee Yun acknowledges the Korea Brain Pool.

Appendix A. Supplementary data

Supplementary data associated with this article can be found, in the online version, at http://dx.doi.org/10.1016/j.snb.2013.01.084.

References

[1] G. Peng, U. Tisch, O. Adams, M. Hakim, N. Shehada, Y.Y. Broza, S. Billan, R. Abdah-Bortnyak, A. Kuten, H. Haick, Diagnosing lung cancer in exhaled breath using gold nanoparticles, Nature Nanotechnology 4 (2009) 669–673.
[2] S. Ampuero, J.O. Bosset, The electronic nose applied to dairy products: a review, Sensors and Actuators B: Chemical 94 (2003) 1–12.
[3] E. Schaller, J.O. Bosset, F. Escher, Practical experience with 'electronic nose' systems for monitoring the quality of dairy products, Chimia 53 (1999) 98–102.
[4] M. Li, E.B. Myers, H.X. Tang, S.J. Aldridge, H.C. McCaig, J.J. Whiting, R.J. Simonson, N.S. Lewis, M.L. Roukes, Nanoelectromechanical resonator arrays for ultrafast, gas-phase chromatographic chemical analysis, Nano Letters 10 (2010) 3899–3903.
[5] M.A. Ryan, M.L. Homer, H. Zhou, K. Manatt, A. Manfreda, A. Kisor, A. Shevade, S.P.S. Yen, Expanding the capabilities of the JPL electronic nose for an international space station technology demonstration, Journal of Aerospace-SAE Transactions 2006-01 (2006) 210–225.
[6] P.-C. Chen, F.N. Ishikawa, H.-K. Chang, K. Ryu, C. Zhou, A nanoelectronic nose: a hybrid nanowire/carbon nanotube sensor array with integrated micromachined hotplates for sensitive gas discrimination, Nanotechnology 20 (2009) 125503.
[7] V.V. Sysoev, J. Goschnick, T. Schneider, E. Strelcov, A. Kolmakov, A gradient microarray electronic nose based on percolating SnO_2 nanowire sensing elements, Nano Letters 7 (2007) 3182–3188.
[8] G. Peng, M. Hakim, Y.Y. Broza, S. Billan, R. Abdah-Bortnyak, A. Kuten, U. Tisch, H. Haick, Detection of lung breast, colorectal, and prostate cancers from exhaled breath using a single array of nanosensors, British Journal of Cancer 103 (2010) 542–551.
[9] M.S. Freund, N.S. Lewis, A chemically diverse conducting polymer-based electronic nose, Proceedings of the National Academy of Sciences of the United States of America 92 (1995) 2652–2656.
[10] Y. Chen, Y. Luo, Precisely defined heterogeneous conducting polymer nanowire arrays—fabrication and chemical sensing applications, Advanced Materials 21 (2009) 2040–2044.
[11] Y. Hu, A.C. To, M. Yun, The controlled growth of single metallic and conducting polymer nanowires via gate-assisted electrochemical deposition, Nanotechnology 20 (2009) 285605.
[12] M. Yun, N.V. Myung, R.P. Vasquez, C. Lee, E. Menke, R.M. Penner, Electrochemically grown wires for individually addressable sensor arrays, Nano Letters 4 (2004) 419–422.
[13] S. Xu, Y. Ding, Y. Wei, H. Fang, Y. Shen, A.K. Sood, D.L. Polla, Z.L. Wang, Patterned growth of horizontal ZnO nanowire arrays, Journal of the American Chemical Society 131 (2009) 6670–6671.
[14] S. Xu, Y. Wei, M. Kirkham, J. Liu, W. Mai, D. Davidovic, R.L. Snyder, Z.L. Wang, Patterned growth of vertically aligned ZnO nanowire arrays on inorganic substrates at low temperature without catalyst, Journal of the American Chemical Society 130 (2008) 14958–14959.
[15] V. Pachauri, A. Vlandas, K. Kern, K. Balasubramanian, Site-specific self-assembled liquid-gated ZnO nanowire transistors for sensing applications, Small 6 (2010) 589–594.
[16] Y. Li, G.W. Meng, L.D. Zhang, F. Phillipp, Ordered semiconductor ZnO nanowire arrays and their photoluminescence properties, Applied Physics Letters 76 (2000) 2011–2013.
[17] Y.-C. Liu, B.-J. Hwang, W.-J. Jian, R. Santhanam, In situ cyclic voltammetry-surface-enhanced Raman spectroscopy: studies on the doping–undoping of polypyrrole film, Thin Solid Films 374 (2000) 85–91.
[18] F. Chen, G. Shi, M. Fu, L. Qu, X. Hong, Raman spectroscopic evidence of thickness dependence of the doping level of electrochemically deposited polypyrrole film, Synthetic Metals 132 (2003) 125–132.
[19] T. Lindfors, A. Ivaska, Raman based pH measurements with polyaniline, Journal of Electroanalytical Chemistry 580 (2005) 320–329.
[20] M.I. Boyer, S. Quillard, E. Rebourt, G. Louarn, J.P. Buisson, A. Monkman, S. Lefrant, Vibrational analysis of polyaniline: a model compound approach, Journal of Physical Chemistry B 102 (1998) 7382–7392.
[21] Y. Hu, D. Perello, U. Mushtaq, M. Yun, A single palladium nanowire via electrophoresis deposition used as a ultrasensitive hydrogen sensor, IEEE Transactions on Nanotechnology 7 (2008) 693–699.
[22] F. Favier, E.C. Walter, M.P. Zach, T. Benter, R.M. Penner, Hydrogen sensors and switches from electrodeposited palladium mesowire arrays, Science 293 (2001) 2227–2231.
[23] T. Gao, E.S. Tillman, N.S. Lewis, Detection and classification of volatile organic amines and carboxylic acids using arrays of carbon black-dendrimer composite vapor detectors, Chemistry of Materials 17 (2005) 2904–2911.
[24] H. Yoon, J. Jang, Conducting-polymer nanomaterials for high-performance sensor applications: issues and challenges, Advanced Functional Materials 19 (2009) 1567–1576.
[25] Z.L. Wang, Nanobelts nanowires, and nanodiskettes of semiconducting oxides—from materials to nanodevices, Advanced Materials 15 (2003) 432–436.
[26] Z. Jing, J. Zhan, Fabrication and gas-sensing properties of porous ZnO nanoplates, Advanced Materials 20 (2008) 4547–4551.
[27] S.T. Shishiyanu, T.S. Shishiyanu, O.I. Lupan, Sensing characteristics of tin-doped ZnO thin films as NO_2 gas sensor, Sensors and Actuators B: Chemical 107 (2005) 379–386.
[28] J.X. Wang, X.W. Sun, Y. Yang, C.M.L. Wu, N–P transition sensing behaviors of ZnO nanotubes exposed to NO_2 gas, Nanotechnology 20 (2009) 465501.

Biographies

Yushi Hu received his BS in Electrical Engineering from the Fudan University, Shanghai, China. He received his MS and Ph.D. degrees in Electrical Engineering from University of Pittsburgh in 2009 and 2011, respectively. He is currently a process engineer in Micron Technology Inc. in Boise, Idaho.

Hyunjoong Lee received the BS, MS, and Ph.D degrees in electrical engineering from Seoul National University (SNU), Seoul, Korea, in 2005 and 2007, respectively. He is currently a postdoctoral reseaercher at the same school. His research interests include sensor interface for MEMS and bio-applications, data converter and analog techniques in CMOS circuits.

Suhwan Kim received the PhD degree in Electrical Engineering and Computer Science from the University of Michigan, Ann Arbor, MI, in 2001. From 2001 to 2004, he was a Research Staff Member in IBM T.J. Watson Research Center, Yorktown Heights, NY. In 2004, Dr. Kim joined Seoul National University, Seoul, Korea, where

he is currently an Associate Professor of Electrical Engineering. His research interests encompass high-performance and low-power analog and mixed signal integrated circuits and technology.

Minhee Yun holds PhD degree from Arizona State University in 1998 and is an associate professor of electrical and computer engineering after four years as a senior staff in the device application group at the Jet Propulsion Laboratory in Pasadena, CA. While at JPL, he led research efforts in the area of device fabrication based on MEMS technologies, and chemical and biochemical nanowire sensor arrays for life detection on Mars and bio-signature detection of emerging diseases. His current research interests include the development of nano-electronic devices for bio-medical applications for early detection of disease signatures using nano-structured materials.